RSC Advances

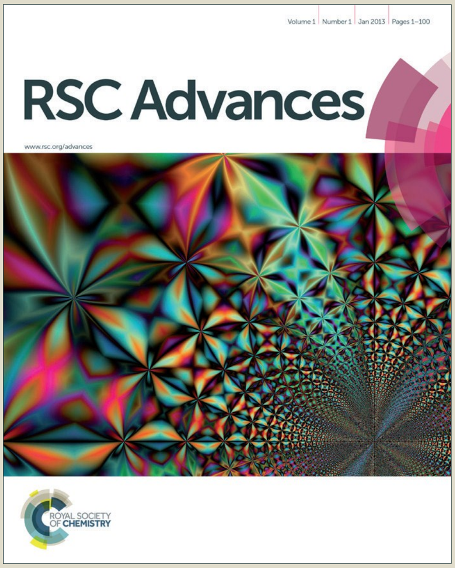

ROYAL SOCIETY OF CHEMISTRY

www.rsc.org/advances

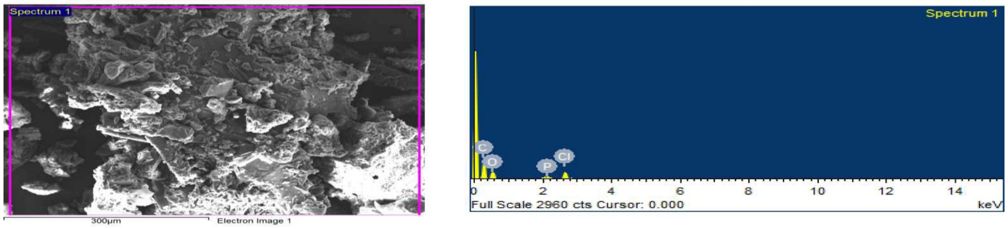

$$\text{MHa-g-poly(HEMA)-PO}_4^{2-}\ 2\text{H}^+ + 2\text{MB}^+ \longrightarrow \text{MHa-g-poly(HEMA)-PO}_4^{2-}\ 2\text{MB}^+ + 2\text{H}^+$$

207x69mm (300 x 300 DPI)

Synthesis and characterization of MHa-g-poly(HEMA)$PO_4^{2-}2H^+$ cation exchanger-effective removal of methylene blue from waste water

Balbir Singh Kaith[a], Jitender Dhiman[a*], Jaspreet Kaur Bhatia[b]

[a] *Department of Chemistry, Dr B.R. Ambedkar National Institute of Technology,*
Jalandhar, 144011, Punjab, India.
[b] Department of Chemistry, Lyallpur Khalsa College, Jalandhar, 144001, Punjab, India

Abstract

Poly(HEMA) chains grafted chemically modified *Holarrhena antidysenterica fiber* was converted into cation-exchanger using phosphorylation and p-doping technique. The cation-exchanger synthesized was found to remove about 94.6% methylene blue dye from aqueous solution. The graft copolymer and cation exchanger vis-a-vis backbone were characterized using different techniques like FTIR, SEM, EDX and XRD. The samples were further evaluated for thermal behavior using TGA/DTA/DTG techniques. The synthesized cation-exchanger was found to possess high thermal stability.

Keywords: Cation exchanger; methylene blue; biodegradable polymer; graft copolymerization; thermal stability

1. Introduction

An exceptional increase in industrial, agricultural and domestic activities has led to increase in water pollutants such as dyes, detergents, insecticides, pesticides and heavy metal ions [1-2]. In industries dyes play an important role in diversified applications like paper colouring, hair colourant, cotton dyeing and wood colouring. More than 0.7 million tons of synthetic dyes are produced all over the world. In paper and textile industries about 10,000 different dyes and pigments are used for colouring purpose. Scientists estimated that about 15% of the total produced synthetic dyes are wasted during processing operations per year which get mixed up with water resources and are hazardous to human health. The non-biodegradable dyes are stable toward photo-chemical effects and are difficult to separate [3-12]. Such accumulation of toxic dyes in water resources causes health problems including heart diseases, vomiting, jaundice, cyanosis, quadriplegia and tissue necrosis [13]. Moreover, the interference of dyes in aquatic system leads to serious problems in the aquatic life cycle. The coloured compounds retard the process of photosynthesis and result in the growth inhibition of aquatic life. The dissolved O_2 concentration in aqueous sources contaminated with toxic dyes also get affected [14-18].

Researchers all over the world are working on the treatment of industrial effluents. A number of methodologies such as adsorption, coagulation, photo-catalysis, chemical precipitation, membrane filtration, reverse osmosis and ion exchange have been developed for the removal of contaminates from water sources. Researchers have been found to use the powdered natural materials as adsorbents for the removal of different types of toxic dyes from waste water [19-24] Ion exchange is one of the important methods which can be used to remove dyes and heavy metal ions from waste water. The ion exchangers have been extensively used for water antibiotic purification and separation of radioisotopes. This method has advantages like large surface area, rapid adsorption and ease of exchange of metal ions. Ion exchangers are found to possess better mechanical, chemical, thermal and radiation stabilities which help them to remain useful under adverse conditions such as boilers and atomic power plants [25-42].

Corresponding author *
E-mail: jitenderdhiman81@gmail.com

Both synthetic and natural backbone can be used in preparation of ion-exchange resins. Since the synthetic materials are not ecofriendly, therefore, attention is focused on the use of natural backbones for the preparation of ion-exchangers. Biopolymers are renewable sources, eco-friendly and get biodegraded at the end of life cycle. A large number of organic polymers such as polyaniline, pectin, cellulose, chitosan, polystyrene and polyacrylamide are used for the preparation of ion-exchangers [43-55].

Ion-absorption capacity of the backbones can be enhanced by the addition of specific functional group. Various methods are available in the laboratory to enhance such properties e.g. thermal, radiation induced modification, plasma treatment, gas-phase oxidation, ultrasonic method and wet chemical or electrochemical oxidation [56-65]. Microwave-induced grafting technique is an effective technique to alter the morphology of polymeric material [66-67]. Desired modification in the materials can be brought about under the influence of microwave radiation [68].

Holarrhena antidysenterica fiber is a bio-polymer which can be converted into ion-exchanger through chemical methods. *H. antidysenterica* is a small to medium-size tree and grows all over India in wild mountains. It is a flowering plant and belongs to *Apocynaceae* family. Its common names are Bitter Oleander, Connessi Bark, Kurchi Bark, Dysentery Rose Bay and Tellicherry Bark. Its stem contains *Kutaja* as one of the ingredients which is used in Ayurveda for the treatment of diarrhoea and dysentery. Scientific studies proved that it also possesses anti-protozoal, anti-giardia and antiamoebic properties. According to Ayurveda the bark of *H. antidysenterica* has anti-diarrhoeal, constipating, astringent, antidysenteric, anthelmintic, carminative and digestive properties [69-72].

Since till date no work on the conversion of H. *antidycentrica* into cation exchanger and its application in the removal of toxic dyes from aqueous medium has been reported in the literature, therefore, the present research work includes the chemical modification of *H. antidycentrica* into a graft copolymer by the incorporation of poly(2-hydroxyethylmethacrylate) chains onto backbone under the influence of microwave radiations and its conversion into cation-exchanger through phosphorylation. The synthesized cation-exchanger was evaluated for its efficiency in removing the dye methylene blue from aqueous medium (Fig.1).

2. Experimental

2.1. Material and Methods

The Holarrhena antidycentrica (Ha) fiber was collected from district Kangra, Himachal Pradesh, India. Ferrous ammonium sulfate (FAS), potassium persulfate (KPS), phosphorous oxychloride and methylene chloride were procured from SD Fine Chemicals. Methylene blue dye was purchased from E-Merk Chemicals.

2.2. Chemical Modification of *Holarrhena antidysenterica* fiber

50 g *of* powdered *H. antidysenterica* plant material was put in cellulosic thimble and was defatted through soxhlet extraction in 500 ml of acetone for 72 hours. The lignins and other undesired impurities were removed from the dried defatted plant material by treating with 40% sodium chlorite solution, maintaining 1:1.5 (mass : volume) for 4 h at 65^0C. pH of the reaction medium was maintained 4.0 by slow addition of acetic acid. The delignified plant material was repeatedly washed with distilled water to ensure the removal of lignins and other soluble

impurities. The resulting plant material was treated with 5% sodium bisulphite solution and final washing was given with distilled water. The modified material was dried in hot air oven at 45^{0}C to ensure the moisture content of 5-10% (Fig. 2a) [73].

2.3. Graft Copolymerization of poly(2-hydroxyethyl methacrylate) chains onto chemically modified *H. antidycetrica*

Chemically modified *H. antidycentrica* (MHa) material was activated by immersing 1.0 g of each sample in distilled water ranging from 6 ml to 18 ml for 24 hours. To each reaction mixture molar ratio of initiator FAS-KPS ranging from 0.3:1.0 to 0.7:1.0 was added followed by the drop wise addition of 0.41 x 10^{-4} to 2.06 x 10^{-4} mol L^{-1} of 2-hydroxyethylmethacrylate and the reaction was carried-out in microwave reactor at a temperature ranging from 50 ^{O}C to 90 ^{O}C, 15 psi pressure and for a time period of 4 to 8 mins. Homo-polymer formed was removed through extraction with dimethylformamide. Graft copolymer was dried at 50^{0}C till constant weight was obtained (Fig. 2b). Percentage graft yield (Pg) was calculated using Eq. 1 [74]:

$$\text{Percentage graft co-polymerization (Pg)} \quad = \quad \frac{W_2 - W_1}{W_1} \text{ x } 100 \qquad (1)$$

Where, W_1 = initial wt. of sample; W_2 = final wt. of sample (after removal of homopolymer).

2.4. Synthesis of [MHa-g-poly(HEMA)$PO_4^{2-}2H^+$] Ion exchanger

MHa-g-poly(HEMA) graft copolymer (1.0 g) was phosphorylized (Fig. 2b) with phosphorous oxychloride (0.8 ml) in pyridine (100 ml) as reaction medium to obtain desired cation-exchanger [75]. The reaction mixture was refluxed using circulating water condenser for 2h at 115^{O}C. After the reaction was completed the product was cooled to 0^{O}C followed by repeated washings with distilled water, 0.1 M HCl and methanol, respectively, in order to remove the traces of pyridine. The product obtained was dried in hot air oven at 50^{O}C. The product was converted to particle size ~ 125 µm and was recovered through sieving. The ~ 125 µm particle sized material was dipped into 100 ml of 1.0 M HNO_3 for 24 hours with occasional shaking and intermittently replacing the supernatant solution with fresh acid for 3 times to convert it into H^+ form. The product was finally washed with distilled water to remove extra acid.

2.4.1. Ion exchange capacity

Cation exchange capacity of MHa-g-poly(HEMA)$PO_4^{2-}2H^+$ was determined with respect to different alkali and alkaline earth metal ions. Glass-wool was kept at bottom of the glass column with internal diameter (i.d.) ~1.5 cm and a bed length of 5.0 cm was prepared using cation-exchanger. Different alkali and alkaline earth metal chlorides were used to equilibrate 5.0 g ion-exchanger with 1.0 mol L^{-1} solution. Flow rate for solution passage was maintained at ~0.5 ml min^{-1} and the collected effluent was titrated against standard 0.1 mol L^{-1} NaOH using phenolphthalein indicator [76].

2.5. Characterization

Agilent Carry 630 Fourier transform infrared (FTIR) spectrometer was used to record the spectra of samples using KBr pellets. SEM-EDX studies of MHa, graft copolymer and cation-exchanger were carried out using FEI Quanta 200 microscope for morphological and elemental analysis of the samples. TGA, DTA and DTG studies were carried-out in air under the temperature range of 50^O–700^OC at a heating rate of 10^OC min^{-1} on TG/DTA 6300, SII EXSTAR 6000. X-ray diffraction studies of the samples were performed on X-ray diffraction instrument (Bruker D8, USA) under ambient conditions using Cu-Kα (1.5418 A^O). The % crystallinity was calculated using Eq. 2 [77]:

$$\%Cr = \frac{I_{22}}{I_{18}+I_{22}} \times 100 \qquad (2)$$

where I_{22} and I_{18} are the crystalline and amorphous intensities at 2θ-scale close to 22° and 18°, respectively

2.6. Swelling studies

The swelling behavior of backbone (MHa), graft copolymer (MHa-g-poly(HEMA)) and cation exchanger (MHa-g-poly(HEMA)$PO_4^{2-}2H^+$) was studied by immersing 0.5 g of each sample in 100 ml of water for 24 hours. The samples were gently wiped-out using filter paper to remove the superficial residual water and the increase in weight of samples was recorded. The percentage swelling was calculated using Eq. 3 [78-79]:

$$\%\ \text{Swelling} = \frac{\text{wt. of swellon polymer} - \text{wt. of dry polymer}}{\text{wt. of dry polymer}} \times 100 \qquad (3)$$

2.7. Dye Removal Studies

Methylene blue dye was used as a model dye to carry-out adsorption studies using cation exchanger in 100 ml flask. 50 ml of methylene blue solution was maintained at a constant temperature to study the effect of contact time and dose of cation-exchanger on the initial concentration of dye. 100-600 mg cation exchanger was used to remove dye from aqua media of concentration 2, 4, 6, 8 and 10 mg L^{-1} at pH 7.0 and $25^{O}C$ for our experimental work. The extent of dye adsorption was determined at different time intervals during adsorption process until equilibrium was attained. Number of replications for each experiment was three. UV spectrophotometer operated at λ_{max} 664 cm^{-1} was used to measure the concentration of dye at different time intervals. The calibration curve was plotted in order to calibrate the instrument to find-out the concentration of unknown samples. Percentage of dye removal was calculated using the Eq. 4 [80]:

$$\% \text{ Dye Removal} = [(C_o - C_{eq})/C_0] \times 100 \qquad (4)$$

Where C_o and C_{eq} are the initial and equilibrium concentration of dye in mg L^{-1}.

2.8 Adsorption Isotherm

The Langmuir isotherm model was used to predict the adsorption of dye methylene blue on the surface of cation exchanger. This model based on the assumption that adsorbate (in liquid, methylene blue) got adsorbed in the form of monolayer on the uniform surface of adsorbent (solid phase, cation exchanger) at a constant temperature and the distribution of the adsobate (methylene blue) between two phases is controlled by equilibrium constant. Thus, at equilibrium the rate of adsorption and desorption is equal [81-82]. The value of q_m and K_L is calculated using Langmuir Eq. 5:

$$\frac{1}{q_e} = \left(\frac{1}{K_L q_m}\right)\frac{1}{C_e} + \frac{1}{q_m} \qquad (5)$$

where q_m= the maximum capacity of adsorption (mg g^{-1}) and K_L = affinity constant of the binding sites (L mg^{-1}); are the Langmuir isotherm constants. q_e= dye adsorbed at equilibrium and C_e= dye concentration at equilibrium

2.8.1 Separation Factor

Separation factor (R_L) is a characteristic of Langmuir isotherm which indicated that whether the adsorption of dye is favorable or not. If the value of R_L =1 then the shape of plot is linear, but if the value of R_L> 1, then the adsorption is unfavorable, whereas, if the value of R_L lies between 0 to 1 the adsorption is favorable, but the value of R_L=0 indicated that the process is irreversible. R_L is dimensionless constant and can be calculated by the Eq. 6 [83]:

$$R_L = \frac{1}{1+K_L C_O} \tag{6}$$

3. Results and Discussion

3.1. Graft copolymerization

Fig. 2 exhibits the mechanism of the incorporation of poly(HEMA) onto H. *antidysenterica* cellulosic backbone through covalent bonding in presence of ferrous ammonium persulphate and potassium persulphate as an initiator system [84-89] . Different reaction parameters were found to affect the percentage grafting. Various reaction conditions such as reaction temperature, time, initiator concentration, monomer concentration and pH were optimized as per the reported work [90-95] to achieve maximum graft yield (422.0%). Optimum reaction conditions obtained were: reaction time, 5 min; reaction temperature, 80^0C; initiator ratio, 0.5:1.0; solvent volume, 10 ml; pH of medium, 7.0 and HEMA, 1.23×10^{-4} mol L^{-1} (Fig. 3a-f). Initially with increase in reaction temperature, reaction time and pH of medium percentage grafting was found to increase upto critical limit. However, further increase resulted in decreased grafting. Initially increase in grafting percentage could be due to the fact that with increase in temperature there was generation of OH* and SO_4^{2-*} which was followed by generation of active sites on the backbone. Live chains on approaching to the backbone active sites get grafted over there resulting in the formation of graft copolymers. However, further increase in temperature and reaction time beyond the optimum, resulted in predominance of homo-polymerization over graft copolymerization. In case of variation in pH of reaction medium, acidic to basic reaction conditions resulted in premature termination of graft copolymerization, thereby giving the decreased graft yield [96]. Reaction parameters like initiator molar ratio, monomer concentration and solvent volume were found to play significant role in grafting process. In the beginning the percentage grafting was found to increase with increase in initiator dose till the optimum ratio (0.5:1.0) was attained. Further increase in initiator concentration resulted in decreased graft yield. This could be due to the reduction of Fe^{3+} ions to Fe^{2+}, thereby resulting in termination of graft copolymerization, hence decreased graft yield [97-98]. The termination of propagating chain reaction can be explained as per the following chemical Eq. 7 [77]:

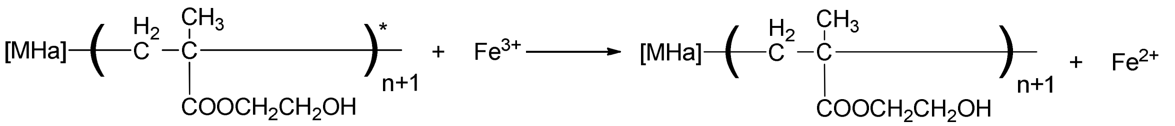

$$[MHa]\left(-\overset{H_2}{C}-\underset{COOCH_2CH_2OH}{\overset{CH_3}{C}}-\right)^{*}_{n+1} + Fe^{3+} \longrightarrow [MHa]\left(-\overset{H_2}{C}-\underset{COOCH_2CH_2OH}{\overset{CH_3}{C}}-\right)_{n+1} + Fe^{2+} \quad (7)$$

Increase in solvent volume beyond optimum value led to decrease in graft yield which was due to the fact that with increase in volume, the concentration of free radicals per unit volume decreased leading to decreased interaction between the active sites of backbone and live chains. Hence, decreased graft yield was observed. Initially graft percentage was found to increase with increase in monomer concentration. However, further increase in monomer concentration beyond optimal resulted in decreased graft yield. This could be due to the occurrence of chain transfer reactions resulting in premature termination of live chains [99]. HEMA has been found to be a potent vinyl monomer for grafting onto bio-polymers and better graft yields have been reported by various workers [100-102]. Grafting of HEMA onto H. *antidysenterica* has been found to give 422.0% graft yield which is quite good in comparison to grafting of HEMA onto other natural backbones. A Comparative study of the graft copolymerization of HEMA onto cellulosics vis-a-vis MHa-g-poly(HEMA) is given in Table 1.

3.2. Ion-exchange capacity

Ion-exchange capacities (IEC) of cation-exchanger with various alkali and alkaline earth metal ions are given in Table 2. Maximum ion-exchange capacity observed was 1.42 mmol g^{-1} for K^{+} ions and 1.31 mmol g^{-1} for Na^{+} ions. Since the Ion-exchange capacity of cation exchanger depends on hydrated radii of metal ions, therefore, smaller the hydrated radii more the ion exchange capacity and the sequence observed accordingly for alkali metal ions was $K^{+} > Na^{+} > Li^{+}$ and in case of alkaline earth metal ions the sequence observed was $Sr^{2+} > Ca^{2+} > Mg^{2+}$ [103]. Comparison of the reported results on ion-exchange capacities of different cation exchangers has shown that poly(methyl methacrylate) Zr(IV) phosphate exhibited higher IEC (2.54 mmol g^{-1})

and followed the order: nylon-6,6 Sn(IV) phosphate (1.98 mmol g^{-1}) > nylon-6,6, Zr(IV) phosphate (1.90 mmol g^{-1}) > acrylamide zirconium (IV) arsenate (1.63 mmol g^{-1}) > acetate–tin (IV) phosphate (1.48 mmol g^{-1}) > poly-o-toluidine Ce(IV) phosphate (1.07 mmol g^{-1}). However, the cation exchanger reported in the present manuscript showed 1.48 mmol g^{-1} IEC which is quite comparable with that of the existing cation exchangers (Table 3) [53, 103-107].

3.3. Fourier transform-infrared (FT-IR)

FTIR spectra of MHa, MHa-g-poly(HEMA) and phosphate cation-exchanger (MHa-g-poly(HEMA)$PO_4^{2-}2H^+$ are shown in Fig. 4. A broad peak at 3330.8 cm^{-1} was observed which was due to the presence of free –OH groups in MHa. Peaks at 2910.0 cm^{-1} and 1021.9 cm^{-1} were due to C-H and C-O stretchings, respectively (Fig. 4a). The IR spectra of MHa-g-poly(HEMA) revealed that there was an increase in the intensity of peak at 1708.8 cm^{-1} which was due to grafting of poly(HEMA) chains containing –C=O functional groups, onto backbone [108]. Decrease in peak intensity at 3363.2 cm^{-1} in IR spectrum of grafted fiber was due to the involvement of free –OH groups in graft copolymerization (Fig. 4c). FTIR spectrum of cation-exchanger MHa-g-poly(HEMA)$PO_4^{2-}2H^+$ also revealed the presence of P=O group by exhibiting peak at 1151.4 cm^{-1} (Fig. 4d) [109]. Reduced intensity of peak corresponding to –OH groups in case of IR spectrum of MHa-g-poly(HEMA)$PO_4^{2-}2H^+$ showed that the phosphorylation involved –OH groups of graft copolymer. Further it has been observed that the absorption ratio of –OH functional groups in case of backbone (MHa), graft copolymer (MHa-g-poly(HEMA)) and cation-exchanger (MHa-g-poly(HEMA)$PO_4^{2-}2H^+$ was found to be 2.8 : 1 : 1.15, respectively, thereby confirming the grafting of poly(2-hydroxyethyl methacrylate) chains on the backbone.

3.4. SEM and Energy-dispersive X-ray (EDX) Studies

SEM and EDX analysis confirmed the successful graft copolymerization of HEMA onto modified plant material. The atomic percentage (Table 4) of carbon (52.97%) and oxygen (47.03%) indicated the cellulosic nature of the modified plant material (Fig 5). SEM images of MHa (Fig. 5a) revealed smooth and homogeneous morphology. The effect of graft copolymerization of HEMA onto MHa was clearly observed in SEM and EDX images of MHa-g-poly(HEMA) (Fig. 5b). These images revealed the information about the increase in roughness and discontinuity of surface. Increased percentage of carbon (57.19%) content and decrease in oxygen (42.81%) content confirms the incorporation of poly(HEMA) chains onto MHa backbone. On the other hand the SEM image of cation-exchanger showed a high degree of heterogeneity. An additional peak of phosphorus (3.21%) with respect to carbon (72.71%) and oxygen (23.86%), was observed in EDX image which indicated the presence of phosphorous in the graft copolymer and the presence of PO_4^{3-} group in the cation-exchanger was confirmed (Fig. 5c).

3.5. X-ray diffraction

XRD patterns of MHa, graft copolymer and cation-exchanger is shown in Fig. 6. MHa fiber showed peak at $21^{O}C$ on 2θ scale (Fig. 6a). % crystallinity of MHa was found to be 47.27%. Peaks of graft copolymer (Fig. 6b) and cation-exchanger (Fig. 6c) were observed at 18^{O} and 9^{O} with percentage crystallinity of 43.43% and 35.88%, respectively. XRD results showed that the crystallinity of MHa decreased after graft copolymerization and its further conversion to cation-exchanger. The introduction of poly(vinyl) chains onto MHa backbone and its further phosphorylation resulted in reduced crystallinity. Decrease in crystallinity was due to disturbance in crystal lattice of MHa by the incorporation of poly(vinyl) chains on the backbone and further functionalization with phosphorylization [77]. A Comparative study of the effect of grafting of HEMA onto bio-polymers vis-a-vis MHa-g-poly(HEMA) and cellulosics is shown in Table 5 [110-112].

3.6. Thermal Studies

Thermogravimetric analysis (TGA) of MHa fiber, graft copolymer and cation exchanger (Table 6) was carried-out as a function of percentage weight loss and temperature [113]. Dehydration, glycogen formation and depolymerization are the processes which take place during the degradation. MHa was found to exhibit two stages of decomposition. First stage was observed in the temperature range between $227.9\text{-}339.7^{O}C$ with 58.2% of weight loss and the second stage from $339.7\text{-}495.9^{O}C$ with 30.6% weight loss. This was due to dehydration, loss of volatile matters and depolymerization processes. Moreover, breakdown of different functional groups like –OH present on the backbone followed by the denaturing of the cyclic rings takes place during second stage decomposition. MHa was found to show 0.287 mg min^{-1} and 0.100

mg min^{-1} rate of weight loss at 300 ^{O}C and 445.6 ^{O}C, respectively. DTA analysis showed exothermic reactions which took place during thermal degradation at 310.4 ^{O}C and 445.5 ^{O}C with the release of 25.8 µV and 20.6 µV energy, respectively (Fig. 7a).

TGA studies of graft copolymer showed one stage decomposition ranging from 205.2-428.8^{O}C. Moreover, the decomposition involves the breaking down of covalent bonding between the poly(vinyl) chains and backbone whereas, the loss of functional groups like –OH and –C=O from the backbone and poly(HEMA) chains takes place during the decomposition with evolution of H_2O vapors and CO_2. Similarly, DTG studies gave clear indication towards the comparatively higher rates of weight loss i. e. 0.852 mg min^{-1}, 0.1479 mg min^{-1} and 0.423 mg min^{-1} at 223.3^{O}C, 271.0^{O}C and 423.0^{O}C, respectively. These observations revealed the fact of decreased thermal stability of graft copolymer in comparison to backbone (Fig. 7b).

Single stage degradation was observed in the TGA studies of phosphorylated ion-exchanger (Fig. 7c). Degradation was observed in the temperature range of 220.8-589.9^{O}C with 85.4% weight loss and the residue left was 7.7%. However, the final decomposition temperature (FDT) was found to be higher in case of cation exchanger in comparison to graft copolymer and backbone indicating the higher thermal stability of the cation exchanger. Rate of weight loss of cation exchanger was observed to be 0.143 mg min^{-1} and 0.273 mg min^{-1} at 268.1 ^{O}C and 542.5 ^{O}C, respectively. Whereas, DTA showed the exothermic reactions during thermal degradation process at 267.3 ^{O}C, 454.2 ^{O}C and 542.5 ^{O}C with 17.9 µV, 24.3 µV and 38.9 µV energy loss, respectively (Table 6) [113-116]. It is evident from the results that though grafting of HEMA onto H. *antidysenterica* cellulosics lead to decrease in thermal stability but conversion of graft copolymer into cation-exchanger through phosphorylation resulted in higher thermal stability. Therefore, the cation-exchanger prepared can work even at higher temperature and is important from technological view point.

3.7. Swelling capacity

The % swelling observed was 238.4%, 126.9% and 176.7% for backbone (MHa), graft copolymer (MHa-g-poly(HEMA)) and cation exchanger (MHa-g-poly(HEMA)$PO_4^{2-}2H^{+}$), respectively. The decrease in % swelling of graft copolymer can be explained on the bases of fact that the hydrophilic sites present on the surface of backbone were blocked due to grafting of poly(HEMA) chain on it. Whereas, an increase in % swelling was observed in case of cation exchanger prepared from graft copolymer, which was due to the fact that in case of cation exchanger there was repulsion between similar charges thereby, creating more space between different chains and hence, more absorption of water [117-120]. It has been observed that though the swelling capacity of the H. *antidysenterica* cellulosics decreased after graft copolymerization with HEMA but the conversion of MHa-g-poly(HEMA) into cation exchanger resulted in higher swelling efficacy. Thus, the cation-exchanger was found to show higher water uptake behavior than the graft copolymer and can be of importance for toxic heavy metal ions removal through adsorption as well as cation exchange processes.

3.8. Dye Adsorption Studies

Cation-exchanger MHa-g-poly(HEMA)$PO_4^{2-}2H^+$ was evaluated for the removal of methylene blue dye from aqueous solution and was found to remove 95.7% dye. Eq. 8 Adsorption action could be due to the electrostatic interactions between PO_3^{2-} groups of cation exchanger MHa-g-poly(HEMA)$PO_4^{2-}2H^+$ and MB=$N^+(CH_3)_2$ groups of MB (Fig. 8). The adsorption process could also take place through the exchange of H^+ ions of cation exchanger with MB=$N^+(CH_3)_2$ of MB dye. Dye adsorption mechanism is depicted in Eq. 9.

Effect of pH on dye sorption can be explained on the basis of mechanism shown in Fig. 8. First step in adsorption is usually deprotonation followed by the formation of X-PO_4^{2-} and $2H^+$. Eq. 9 and Eq. 11 showed the adsorption of methylene blue on the surface of cation exchanger due to electrostatic interactions. As we raise the pH of reaction medium, the production of large number of X-PO_4^{2-} species took place which facilitated the adsorption of MB dye on the surface of cation exchanger. Further, MB^+ can also get adsorbed on the cation exchanger through ion exchange process between MB^+ and H^+. pH higher than neutral led to facilitate the Eq. 10 and Eq. 15 but does not facilitate the Eq. 13 which leads to decrease in adsorption capacity of the cation-exchanger [121].

3.8.1. Effect of initial concentration of dye

The effect of Initial concentration of dye was studied as a function of time of contact with cation-exchanger (Fig. 9a). Different methylene blue solutions with initial concentration 2 mg L^{-1}, 4 mg L^{-1}, 6 mg L^{-1}, 8 mg L^{-1} and 10 mg L^{-1} were allowed to undergo cation exchange process and adsorption with fixed amount of cation exchanger (500 mg/ 50 ml of MB) till saturation point was reached. The maximum time of contact was found to be 225 min. Percentage of dye removal is depicted in Fig 9a. Initially with increase in concentration of MB there was an increase in percentage of dye removal from 73.68% to 84.62%. This could be either due to increase in interaction of dye with adsorbent or ion exchange process. On further increase in the concentration of dye from 4 mg L^{-1} to 10 mg L^{-1} a decrease in the rate of dye removal from 84.62% to 69.31% was found. This decrease in the rate of dye removal from aqueous medium was due to decrease in ion-exchange capacity of adsorbent. This can be explained on the basis of the fact that with the increase in the dye concentration active sites on adsorbent for dye removal decreases and hence decrease in dye-adsorbent interaction. Thus, at low concentration of MB i.e. from 2 mg L^{-1} to 4 mg L^{-1}, the presence of dye removal was higher as compare to MB concentration with 4 mg L^{-1} to 10 mg L^{-1} [122].

3.8.2. Effect of the time on dye removal

Studies on the removal of methylene blue dye from the aqueous medium using cation exchanger were carried-out as a function of contact time (Fig. 9a). It has been observed that dye removal process involved three phases. First phase showed a sharp increase in graph slope during the initial time interval upto 20 min. Afterward the rate of dye removal was found to decrease with time interval till the equilibrium was attained. Enhanced initial rate of dye uptake was due to the presence of a large number of vacant sites on cation exchanger and dye removal was observed to occur due to adsorption through ionic interaction as well as through ion-exchange process. Later phase of slow adsorption can be attributed to intra-particle diffusion which is a slow process. In final stage of adsorption the constant values obtained showed that the diffusion which occurred through small pores of adsorbent led to equilibrium between adsorbate and adsorbent. Moreover, final stage includes the saturation of vacant sites and thus showed a constant slope of curve. The equilibrium point was attained at 80 min, 110 min, 140 min, 180 min and 200 min in case of methylene blue dye solution with concentration of 2 mg L^{-1}, 4 mg L^{-1}, 6 mg L^{-1}, 8 mg L^{-1} and 10 mg L^{-1}, respectively. However maximum dye removal (73.68% to 84.62 %) was observed at 110 min time interval with 4 mg L^{-1} dye concentration [123].

3.8.3. Effect of adsorbent dose

Impact of adsorbent dose on dye adsorption was studied by varying the dose from 100 mg to 600 mg while keeping all other parameters constant (Fig. 9b). Initially an increase in dye adsorption (60.0%- 94.6%) was observed with increase in adsorbent dose from 100 mg/ 50 ml of MB to 500 mg/ 50 ml of MB. This was due to increase in availability of active sites which enhanced the percentage adsorption of dye. Further increase in adsorbent dose resulted in decreased rate of dye removal from the aqueous medium. This decrease in the rate of adsorption is attributed to aggregation of adsorption sites with decreased vacant sites surface area available for dye adsorption and increased diffusion path length. Adsorbent dose beyond optimal and the diffusion path length are directly proportional. Hence, the increased dose beyond optimum concentration resulted in decreased adsorption of methylene blue dye along with delayed equilibrium [123].

3.9 Langmuir isotherm

Fig. 10 shows the linear fit graph of Langmuir isotherm for the adsorption of methylene blue on the surface of cation exchanger MHa-g-poly(HEMA)$PO_4^{2-}2H^+$ at 25^OC. Table 7 represents the calculated values of q_m, K_L and R^2 using Langmuir isotherm. The calculated value of R^2 from Langmuir isotherm is 0.9881 which is quite high. Moreover, if the value of R^2 comes higher than 0.89 in that case the adsorption data would follow the Langmuir isotherm. The maximum adsorption capacity (q_m) of cation exchanger calculated from isotherm was found to be 3.12 mg g^{-1} of material and the value of K_L was 0.076 L mg^{-1} as shown in Table 7. Since the adsorption data followed the Langmuir isotherm which revealed the fact that the surface of cation exchanger was homogeneous and MB dye was adsorbed in the form of monolayer at the outer surface of the cation exchanger [124-128].

3.9.1 Separation Factor

The value of separation factor (R_L) was calculated using the value of K_L which was obtained from the Langmuir isotherm. The adsorption process of methylene blue dye on the surface of cation-exchanger was favorable as the calculated value of $R_L = 0.767$ which is less than 1 [125, 129].

4. Conclusion

Property profile of the chemically modified *H. antidysenterica fiber* was enhanced with the incorporation of poly(HEMA) chains through graft copolymerization and further its conversion to cation exchanger on phosphorylation and doping with 1.0 M HNO_3. Cation exchanger synthesized was found to remove 94.6% methylene blue dye from aqueous medium. Concentration of dye solution, adsorbent-adsorbate contact period and adsorbent dose were found to have significant role in dye adsorption process. Hence, the cation exchanger prepared from natural backbone is important from technology view point for the treatment of waste water.

Acknowledgements

Authors are highly grateful to DST-FIST New Delhi for providing financial assistance for the procurement of equipment used in the characterization of the samples. Authors are also thankful to IIT Roorkee for the SEM and EDX analysis of the samples.

References

[1] R. Jiraratananon, A. Sungpet and P. Luangsowan, *Desalination*, 2000, 130, 177-183.

[2] A. Bhatnagar and M. Sillanpaa, *Adv. Colloid Interface Sci.*, 2009, 152, 26–38.

[3] N. Koprivanac and H. Kusic, Hazardous organic pollutants in colored wastewaters, *Nova Science Publishers*, New York, 2008.

[4] N. M. Mahmoodi and M. Arami, *J. Appl. Polym. Sci.*, 2008, 109, 4043–4048.

[5] N. M. Mahmoodi and M. Arami, *Chem. Eng. J.*, 2009, 146, 189–193.

[6] L. Curkovic, D. Ljubas, S. Segota and I. Bacic, *J. Alloys Compd.*, 2014, 604, 309–316.

[7] T. S. Natarajan, H. C. Bajaj and R. J. Tayade, *J. Colloid Interface Sci.*, 2014, 433, 104–114.

[8] M. Visa, C. Bogatu and A. Duta, *Appl. Surf. Sci.*, 2010, 256, 5486–5491.

[9] R. Y. Lin, B. S. Chen, G. L. Chen, J. Y. Wu, H. C. Chiu and S. Y. Suen, *J. Membr. Sci.*, 2009, 326, 117–129.

[10] B. S. Rathore and D. Pathania, *J. Alloys Compd.*, 2014, 606, 105–111.

[11] S. M. Al-Rashed and A. A. Al-Gaid, *J. Saudi Chem. Soc.*, 2012, 16, 209–215.

[12] H. Demir, A. Top, D. Balkose and S. Ulku, *J. Hazard. Mater.,* 2008, 153, 389–394.

[13] Y. H. Gad, *Radiat. Phys. Chem.*, 2008, 77, 1101– 1107.

[14] M. Naushad, *Chem. Eng. J.,* 2014, 235, 100–108.

[15] M. E. Argun, *J. Hazard. Mater.,* 2008**,** 150, 587–595.

[16] S .A. Nabi and M. Naushad, *Colloids Surf., A, 2007,* 293, 175–184.

[17] Z. A. Alothman, M. M. Alam and M. Naushad, *J. Ind. Eng. Chem.,* 2013, 19, 956–960.

[18] M. Naushad, Z. A. Alothman and M. Islam, *Int. J. Environ. Res. Publ. Health.,* 2013, 10, 567–578.

[19] A. Mirmohseni, M. S. Seyed Dorraji, A. Figoli and F. Tasselli, *Bioresour. Technol.*, 2012, 121, 212–220.

[20] B. H. Hameed**,** *J. Hazard. Mater.*, 2009, 161, 753-759.

[21] F. Deniz and S. Karaman, *Chem. Eng. J.*, 2011, 170, 67–74.

[22] S. Dawood and T. K. Sen, *Water Res.,* 2012, 46, 1933-1946.

[23] C. Namasivayam and N. Kanchana, *Chemosphere*, 1992, 25, 1691–1705

[24] R. Jain and M. Shrivastava, *J. Hazard. Mater.*, 2008, 158, 549–556.

[25] M. M. Alam, Z. A. Alothman and M. Naushad, *J. Ind. Eng. Chem.*, 2013, 19, 1973–1980.

[26] Z. A. Al-Othman, M. Naushad and A. Nilchi, *J. Inorg. Organomet. P.*, 2011, 21, 547-559.

[27] Z. A. AL-Othman, M. Naushad and Inamuddin, *Chem. Eng. J.*, 2011, 172, 369-375.

[28] A. A. Khan, Inamuddin and M. M. Alam, *React. Funct. Polym.,* 2005, 63, 119-133.

[29] A. A. Khan and Inamuddin, *J. Appl. Polym. Sci.*, 2007, 105, 2806-2815.

[30] J. Zhang, B. Li, Z. Wang, G. Cheng, S. Dong and Anal. Chim. *Acta.*, 1999, 388, 71-78.

[31] S. Deng, C. Wang, Y. Zhou, F. Huang and L. Du, *Mater Sci Eng.*, 2008, 477, 96-99.

[32] B.P. Tripathi and V.K. Shahi, *Prog. Polym. Sci.*, 2011, 36, 945-979.

[33] D. Pathania, G. Sharma, M. Naushad and A. Kumar, *J. Ind. Eng. Chem.,* 2014, 20, 3596–3603.

[34] J. B. Rivest and P. K. Jain , *Chem. Soc. Rev.*, 2013,42, 89-96.

[35] C. K. Brozek and M. Dinca, *Chem. Soc. Rev.*, 2014, 43, 5456-5467.

[36] K. Bunzl and B. Sansoni, *Chemie Ingenieur Technik,* 1975, 47, 925-934.

[37] Atsushi Tsuji, Hiroaki Takahashi and Takao Oi, *J. Mater. Chem.*, 2003, 13, 542-549.

[38] X. H. Qi, K. Z. Du, M. L. Feng, J. R. Li, C. F. Du, B. Zhang and X. Y. Huang, *J. Mater. Chem. A*, 2015.

[39] H. Takahashi, Y. H. Zhang, T. Miyajima and Takao Oi, *J. Mater. Chem.*, 2006, 16, 1462-1469.

[40] A. A. Khan and S. Shaheen, *RSC Adv.*, 2014, 4, 23456-23463.

[41] A. Dyer, M. Pillinger and S. Amin, *J. Mater. Chem.*, 1999, 9, 2481-2487.

[42] B. Paull and W. Bashir, *Analyst*, 2003, 128, 335-344.

[43] A. Ozer and G. Dursan, *J. Hazard. Mater., 2007,* 146, 262–269.

[44] Z. A. AL-Othman, M. Naushad and A. Nilchi, *J. Inorg. Organomet. Polym.* 2011, 21, 547-559.

[45] P. Zhang, H. H. Hahn and E. Hoffmann, *Acta Hydrochim. Hydrobiol.*, 2003, 31, 145-151.

[46] V. K. Gupta, D. Pathania, N. C. Kothiyal and G. Sharma, *Carbohydr. Polym.,*2013, 96, 277-283.

[47] L. K. Wang, Y. T. Hung and N. K. Shammas, *Springer*, New York City, 2005.

[48] M. E. Ersahin, H. Ozgun, R. K. Dereli, I. Ozturk and K. Roest, *Bioresour. Technol.,* 2012, 122, 196-206.

[49] A. Bodalo-Santoyo, J. L. Gomez-Carrasco, E. Gomez-Gomez, F. Maximo-Martin and A. M. Hidalgo-Montesinos, *Desalination*, 2003, 155, 101–108.

[50] A. Nilchi, R. Saberi, H. Azizpour, M. Moradi, R. Zarghami and M. Naushad, *Chem. Ecol.*, 2012, 28, 169-185.

[51] V. S. Soldatov, A. A. Shunkevich, I. S. Elinson, J. Johann and H. Iraushek, *Desalination,* 1999, 124, 181–192.

[52] X. Chunhua and Y. Caiping, *J. Hazard. Mater.,* 2009, 170, 1125–1132.

[53] Inamuddin, S. A. Khan, W. A. Siddiqui and A. A. Khan, 2007, *Talanta*, 71, 841-847.

[54] C. S. Sundaram and S. Meenakshi, *J. Colloid Interface Sci.*. 2009, 333, 58–62.

[55] M. Islam and R. Patel, *J. Hazard. Mater.,* 2008, 156, 509–520.

[56] A. Bismarck, C. Wuertz and J. Springer, *Carbon*, 1999, 37, 1019-1027.

[57] T. Ramanathan, A. Bismarck, E. Schulz and K. Subramanian, *Compos. Sci. Technol.*, 2001, 61, 1703–1710.

[58] A. P. Kettle, A. J. Beck, L. O. Toole and F. R. Jones, *Compos. Sci. Technol.,* 1997, 57, 1023–1032.

[59] M. A. Montes-Moran, A. Martinez-Alonso, J. M. D. Tascon and R. J. Young, *Composites Part A,* 2001, 32, 361–371.

[60] X. L. Fu, W. M. Lu and D. D. L. Chung, *Carbon,* 1998, 36, 1337–45.

[61] H. Zhang, Z. Zhang and C. Breidt, *Compos. Sci. Technol.*, 2004**,** 64, 2021–2029.

[62] Y. D. Huang, L. Liu, J. H. Qiu and L. Shao, *Compos. Sci. Technol.*, 2002, 62, 2153–2159.

[63] B. S. Kaith, S. Kalia, *Polym. J.,* 2007, 39, 1319-1327.

[64] B. S. Kaith, R. Jindal and M. Maiti, *Int. J. Polym. Anal. Charact.* 2009, 14, 210 - 230.

[65] H. L. Cao, Y. D. Huang and Z. Q. Zhang, *Compos. Sci. Technol.*, 2005, 65, 1655–1662.

[66] R. L. Clough, *Nucl. Instrum. Methods Phys. Res., Sect. B.*, 2001, 185, 8–23.

[67] C. O. Kappe, *Angew. Chem. Int. Ed.*, 2004, 43, 6250–6284.

[68] S. Machi, *Radiat. Phys. Chem.*, 1996, 47, 333–410.

[69] India, Ministry of Health and Family Welfare, The Ayurvedic pharmacopoeia of India. Part I, *New Delhi: Department of Indian Systems of Medicine & Homeopathy*, 2001, 1, 78-79.

[70] India, Ministry of Health and Family Welfare, The Ayurvedic formulary of India, *New Delhi: Department of Indian Systems of Medicine & Homeopathy Part-II*, 2000, 35-66.

[71] P. C. Sharma, M. B. Yelne and T. J. Dennis, *Data base on medicinal plants used in Ayurveda. New Delhi: Central Council for Research in Ayurveda & Siddha*, 2002, 2, 349.

[72] P. C. Sharma, M. B. Yelne and T. J. Dennis, *Data base on medicinal plants used in Ayurveda. New Delhi: Central Council for Research in Ayurveda & Siddha . New Delhi: Central Council for Research in Ayurveda & Siddha*, 2001, 2, 348.

[73] H. Chattopadhyay and P. B. Sarkar, *Proc. Indian Nat. Sci. Acad. Part A, 1946,* 12, 23-46.

[74] B. S. Kaith, R. Jindal and J. K. Bhatia, *J. Appl. Polym. Sci.*, 2011, 120, 2183–2190.

[75] J. Lehrfeld, *J. Appl. Polym. Sci.*, 1996, 61, 2099–2105.

[76] S. A. Nabi, Alimuddin and A. Islam, *J. Hazard. Mater.*, 2009, 172, 202-207.

[77] B. S. Kaith, R. Jindal, A. K. Jana and M. Maiti, *Carbohydr. Polym.,* 2009, 78, 987–996.

[78] M. M. Mishra, M. Yadav, A. Sand, J. Tripathy and K. Behari, *Carbohydr. Polym.*, 2000, 80, 235–241.

[79] H. A. A. EL-Rehim, A. H. EL-Sayed and A. M. Ali, *J. Appl. Polym. Sci.*, 2000, 76, 125–132.

[80] L. Fana, Y. Zhangb, X. Li, C. Luoa, F. Lua and H. Qiua, *Colloids Surf., B.,* 2012, 91, 250–257.

[81] G. Annadurai, S. R. Juang and J. D. Lee, *J. Hazard. Mater.*, 2002, 92, 263-274.

[82]Y. S. Ho, W. T. Chiu and C. C. Wang, *Bioresour. Technol.*, 2005, 96,1285-1291.

[83] T. M. Elmorsi, *Journal of Environmental Protection*, 2011, 2, 817-827

[84] V. K. Thakur, M. K. Thakur and R. K. Gupta, *Carbohydr. Polym.*, 2013, 98, 820–828.

[85] V. K. Thakur, M. K. Thakur and R. K. Gupta, *Int. J. Biol. Macromol.*, 2013, 62, 44–51.

[86] P. Lv, Y. Bin, Y. Li, R. Chen, X. Wang and B. Zhao, *Polymer*, 2009, 50, 5675–5680.

[87] A. Das and C. N Saikia, *Bioresour. Technol.*, 2000, 74, 213–216.

[88] I. Kaur, R. Kumar and N. Sharma, *Carbohydr. Res.*, 2010, 345, 2164–2173.

[89] M. H. El-Rafie, M. K. Zahran and A. Hebeish, *Polym. Degrad. Stab.*, 1993, 42, 223–230.

[90] Y. Liu, Y. Zhang, Z. Liu and K. Deng, *Eur. Polym. J.*, 2002, 38, 1619–1625.

[91] K. Behari, P. K Pandey, R. Kumar and K. Taunk, *Carbohydr. Polym.*, 2001, 46, 185–189.

[92] J. R. Witono, I. W. Noordergraaf, H. J. Heeres and L. P. B. M. Janssen, *Carbohydr. Polym.*, 2012, 90, 1522–1529.

[93] A. A. Al-Hoqbani, E.S. Abdel-Halim and S. S. Al-Deyab, *Int. J. Biol. Macromol.*, 2014, 70, 275–283.

[94] J. Tripathy, D. K. Mishra and K. Behari, *Carbohydr. Polym.*, 2009, 75,604–611.

[95] A. S. Singha and R. K. Rana, *Carbohydr. Polym.*, 2012, 87, 500–511.

[96] B. S. Kaith, R. Jindal and M. Maiti, *J. Appl. Polym. Sci.,* 2009, 113, 1781-1791.

[97] B. S. Kaith, J. K. Bhatia, J. Dhiman, R. Singla, P. Mehta, V. Yadav and S. Bhatti, *Polym. Bull.,* 2013, 70, 3155-3169.

[98] D. Roy, M. Semsarilar, J. T. Guthrie and S. Perrier, *Chem. Soc. Rev.*, 2009, 38, 2046-2064.

[99] H. H. Sokker, N. M. El-Sawy, M. A. Hassan and B. E. El-Anadouli, *J. Hazard. Mater.*, 2011, 190, 359–365.

[100] J. M. Joshi and V. K. Sinha, Graft copolymerization of 2-hydroxyethylmethacrylate onto carboxymethyl chitosan using CAN as an initiator, *Polymer*, 2009, 47, 2198–2204.

[101] J. L. Rivera-Armenta, C. G. Flores-Hernandez, R. Z. D. Angel-Aldana, A. M. Mendoza-Martinez, C. Velasco-Santos and A. L. Martinez-Hernandez, ed. T. Theophile, *InTech*, 2012, ch. 12, 245-260.

[102] I. M. El-Sherbinya and H. D.C. Smyth, *Carbohydrate Polymers*, 2010, 81, 652–659.

[103] W. A. Siddiqui, S. A. Khan and Inamuddin, *Colloids Surf., A.*, 2007, 295, 193-199.

[104] S. A. Nabi and A. H. Shalla, *J. Hazard. Mater.*, 2009, 163, 657–664.

[105] A. A. Khan and T. Akhtar, *Solid State Sci.*, 2011, 13, 559-568.

[106] B. S. Rathore, G. Sharma, D. Pathania and V. K. Gupta, *Carbohydr. Polym.*, 2014, 103, 221-227.

[107] A. A. Khan and T. Akhtar, *Electrochim. Acta*, 2009, 54,3320–3329.

[108] C. He, M. Wang, X. Cai, X. Huang, L. Li, H. Zhu, J. Shen and J. Yuan, *Appl. Surf. Sci.*, 2011, 258, 755– 760.

[109] S. A. Nabi, A. Akhtar, M. D. A. Khan and M. A. Khan, *Desalination*, 2014, 340, 73–83.

[110] A. Sh. Goikhman, V. M. Irklei, O. S. Vavrinyuk and V. I. Pirogov, *Fibre Chemistry*, 1992, 24, 80-85.

[111] N. Terinte, R. Ibbett and K. C. Schuster, *Lenzinger Berichte*, 2011, 89, 118-131.

[112] B. S. Kaith, J. Dhiman and Jaspreet Kaur Bhatia, Journal of Environmental Chemical Engineering, 2015 (in press)

[113] E. Princi, S. Vicini, E. Pedemonte, A. Mulas, E. Franceschi, G. Luciano and V. Trefiletti, *Thermochim. Acta*, 2005, 425, 173–179.

[114] J. F. Mano, D. Koniarova and R. L. Reis, *J. Mater. Sci.: Mater. Med.*, 2003, 14, 127-135,

[115] H. Lonnberg, L. Fogelstrom, M. A. S. A. Samir, L. Berglund, E. Malmstrom and A. Hult, *Eur. Polym. J.*, 2008, 44, 2991–2997.

[116] M. J. Zohuriaan and F. Shokrolahi, *Polym. Test.,* 2004, 23, 575–579.

[117] D. K. Mishra, J. Tripathy and K. Behari, *Carbohydr. Polym.*, 2008, 71, 524–534.

[118] F. Madsen and N. A. Peppas, *Biomaterials*, 1999, 20, 1701–1708.

[119] S. Kim, J. H. Kim and D. Kim, *J. Colloid Interface Sci.,* 2011, 356, 100–106.

[120] Q. Li, Z. Ma, Q. Yue, B. Gao, W. Li and X. Xu, *Bioresour. Technol.*, 2012, 118, 204–209

[121] C.H. Weng and Y.F. Pan, J. Hazard. Mater. 144, 2007, 355–362.

[122] A. T. Paulino, M. R. Guilherme, A. V. Reis, G. M. Campese, E. C. Muniz and J. Nozaki, *J. Colloid Interface Sci*., 2006, 301, 55-62.

[123] E. S. Abdel-Halim, *React. Funct. Polym.,* 2013, 73, 1531–1536.

[124] A. S. Alzaydien, *American Journal of Applied Sciences*, 2009, 5,197-208.

[125] B. H. Hameed, A. T. M. Din and A. L. Ahmad, *J. Hazard. Mater.,* 2007, 141, 819-825.

[126] W. T. Tsai, C. Y. Chang, M. C. Lin, S. F. Chien, H. F. Sun and M. F. Hsieh, *Chemosphere*, 2001, 45, 51-58.

[127] P. K. Malik, *J. Hazard. Mater.,* 2004, 113, 81-88.

[128] C. Namasivayam and D. Kavitha, *Dyes Pigm.,* 2002, 54, 47-58.

[129] N. T. Abdel-Ghani, R. M. El-Nashar and G. A. El-Chag-haby, *Elec. J. Env. Agricult. Food Chem.*, 2008, 7, 3126-3133.

Figure legends

Fig. 1: Structure of methylene blue

Fig. 2: Schematic representation of (a) Chemical modification of H. antidysenterica fiber (b) synthesis of graft copolymer and phosphate cation-exchanger

Figs. 3a-f: Effect of (a) reaction time (b) reaction temperature (c) initiator ratio (d) solvent concentration (e) pH of medium (f) monomer concentration on graft yield

Figs. 4a-c: FT-IR spectra of (a) MHa (Modified *H. antidysenterica* fiber) (b) MHa-g-poly(HEMA) (c) MHa-g-poly(HEMA)PO_4^{2-} $2H^+$

Figs. 5a-a_1 to c-c_1: SEM-EDX of (a-a_1) MHa-Fiber (b-b_1) MHa-g-poly(HEMA) (c-c_1) MHa-g-poly(HEMA)$PO_4^{2-}2H^+$

Figs. 6a-c: XRD pattern of (a) MHa-Fiber (b) MHa-g-poly(HEMA) (c) MHa-g-poly(HEMA)$PO_4^{2-}2H^+$

Figs. 7a-c: TGA/DTA/DTG of (a) MHa-Fiber (b) MHa-g-poly(HEMA) (c) MHa-g-poly(HEMA)$PO_4^{2-}2H^+$

Figs. 8a-b: (a) Electrostatic interaction and cation (b) exchange reaction between phosphate resin and methylene blue (c-h) effect of pH on dye adsorption

Figs. 9a-b: Effect of (a) contact time and initial concentration of dye (b) dose of cation exchanger on % dye removal

Fig 10: Langmuir adsorption isotherm

Table legends

Table 1: Comparitive study of the graft copolymerization of HEMA onto cellulosics vis-a-vis MHa-g-poly(HEMA)

Table 2: Ion-exchange capacity of various exchanging ions on phosphate cation-exchanger

Table 3: Comparison between the ion-exchange capacity of various cation exchangers to MHa-g-poly(HEMA)$PO_4^{2-}2H^+$ cation exchanger

Table 4: Comparison between the atomic percentage of MHa, MHa-g-poly(HEMA) and MHa-g-poly(HEMA)$PO_4^{2-}2H^+$

Table 5: Comparative study of the effect of grafting of HEMA onto bio-polymers on % crystallinity vis-a-vis MHa-g-poly(HEMA) and cellulosics

Table 6: Thermal studies of MHa, MHa-g-poly(HEMA) and MHa-g-poly(HEMA)$PO_4^{2-}2H^+$

Table 7: Parameters of Langmuir isotherm

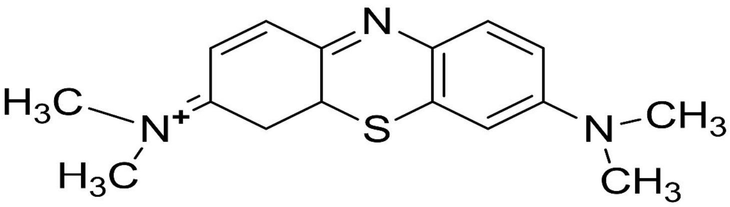

Fig. 1

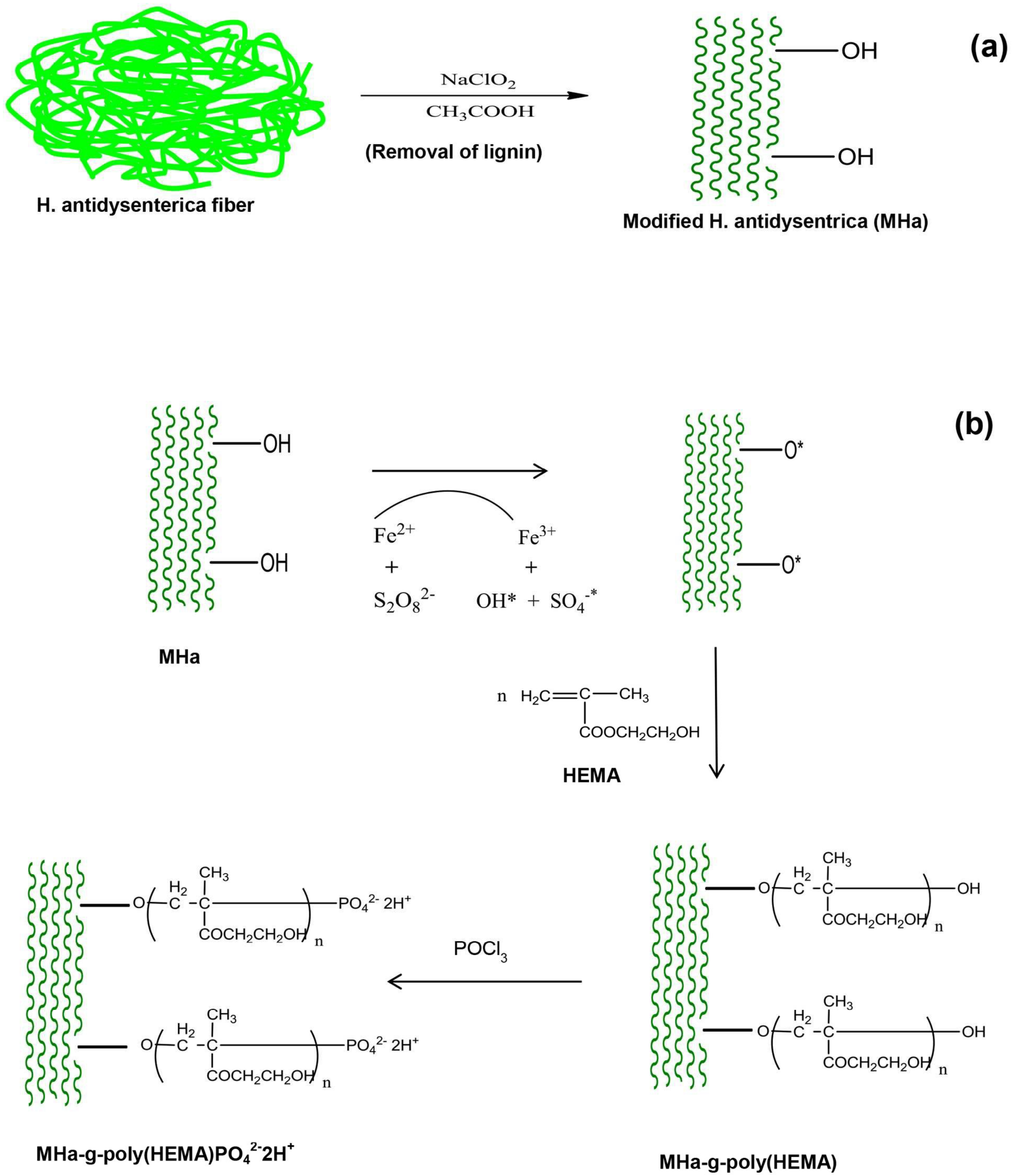
(a)
H. antidysenterica fiber
NaClO2
CH3COOH
(Removal of lignin)
OH
OH
Modified H. antidysentrica (MHa)
(b)
OH
OH
MHa
Fe2+
+
S2O82-
Fe3+
+
OH* + SO4-*
O*
O*
n H2C=C—CH3
COOCH2CH2OH
HEMA
POCl3
MHa-g-poly(HEMA)PO42-2H+
MHa-g-poly(HEMA)

Fig. 2

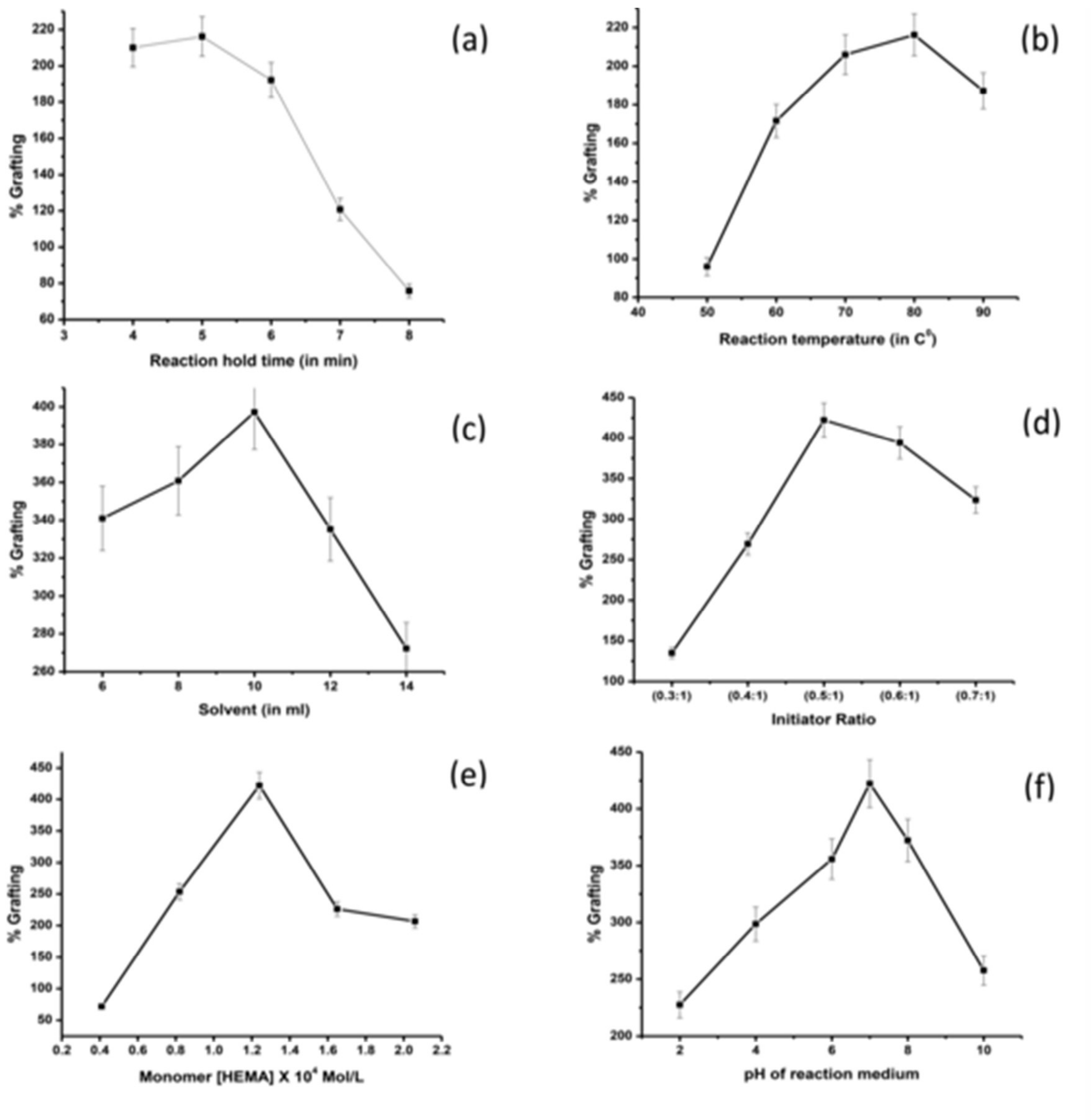
(a)
220
200
180
160
140
120
100
80
60
% Grafting
3
4
5
6
7
8
Reaction hold time (in min)
(b)
220
200
180
160
140
120
100
80
% Grafting
40
50
60
70
80
90
Reaction temperature (in C^0)
(c)
400
380
360
340
320
300
280
260
% Grafting
6
8
10
12
14
Solvent (in ml)
(d)
450
400
350
300
250
200
150
100
% Grafting
(0.3:1)
(0.4:1)
(0.5:1)
(0.6:1)
(0.7:1)
Initiator Ratio
(e)
450
400
350
300
250
200
150
100
50
% Grafting
0.2
0.4
0.6
0.8
1.0
1.2
1.4
1.6
1.8
2.0
2.2
Monomer [HEMA] X 10^4 Mol/L
(f)
450
400
350
300
250
200
% Grafting
2
4
6
8
10
pH of reaction medium

Fig. 3

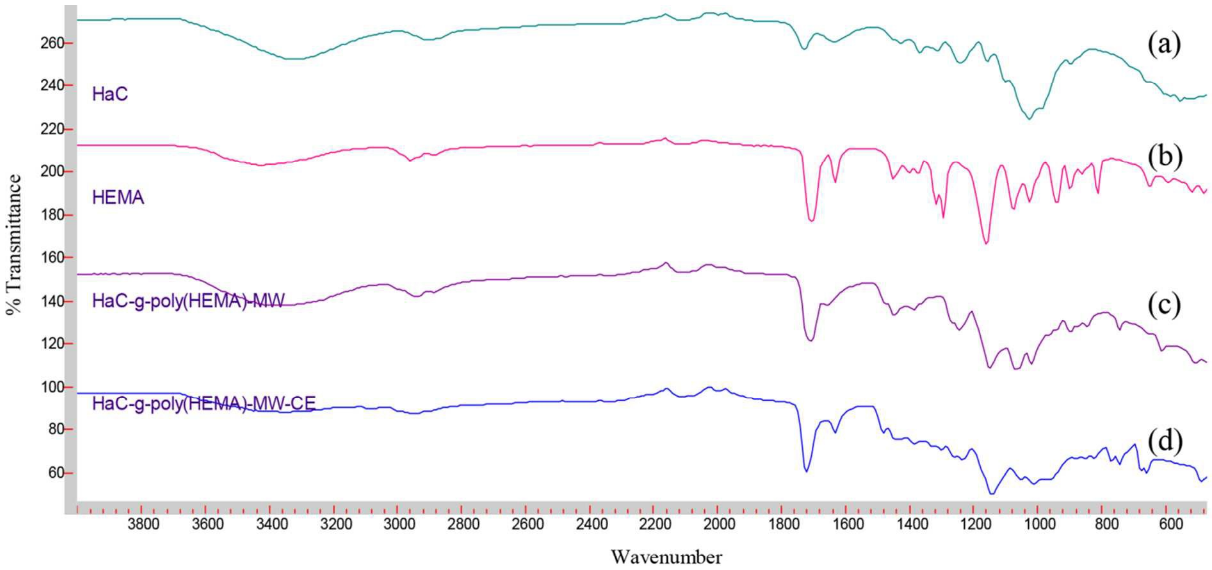
% Transmittance
260
240
220
200
180
160
140
120
100
80
60
HaC
HEMA
HaC-g-poly(HEMA)-MW
HaC-g-poly(HEMA)-MW-CE
(a)
(b)
(c)
(d)
3800
3600
3400
3200
3000
2800
2600
2400
2200
2000
1800
1600
1400
1200
1000
800
600
Wavenumber

Fig 4

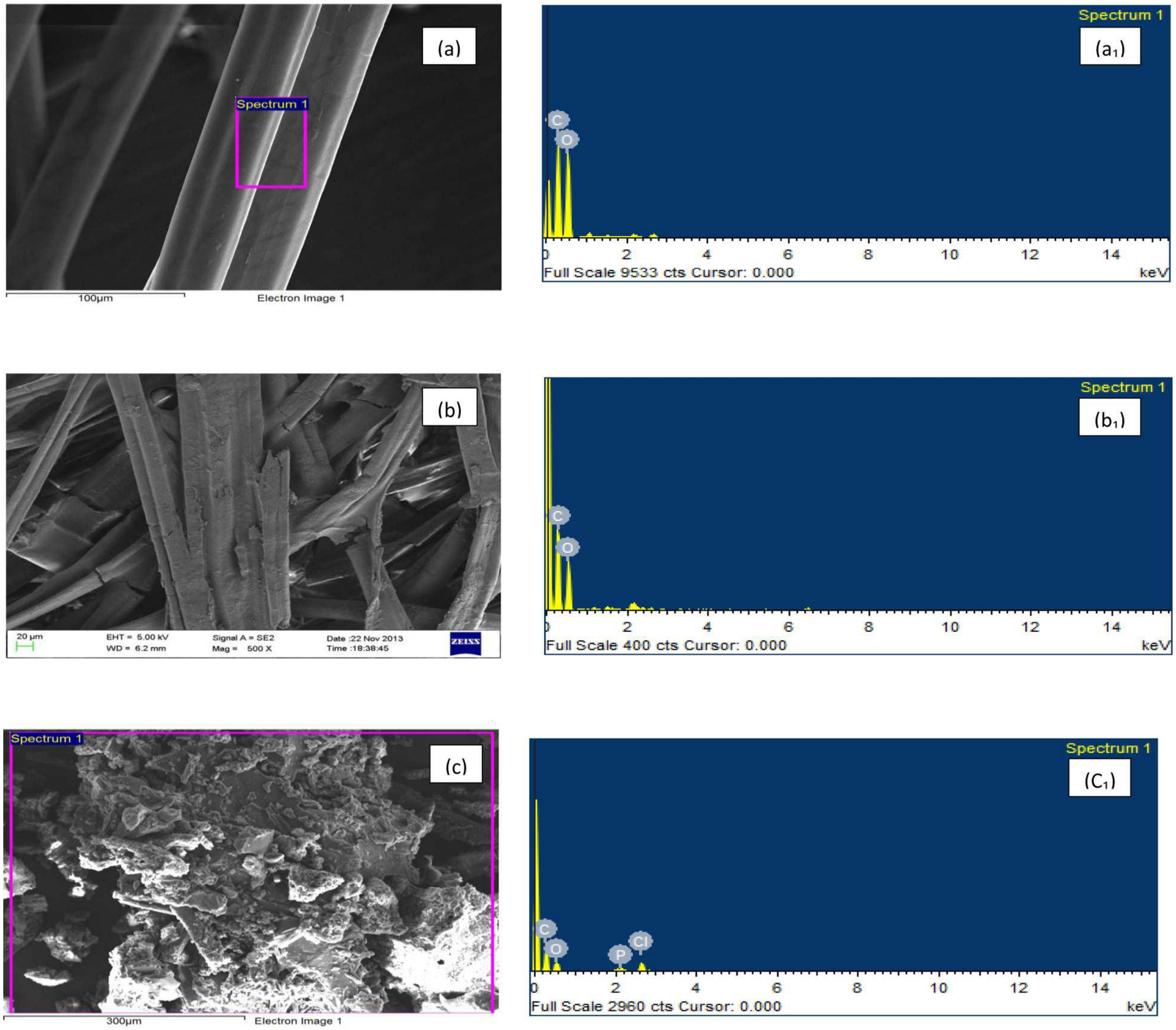
(a)
Spectrum 1
100µm
Electron Image 1
Spectrum 1
(a$_1$)
C
O
0 2 4 6 8 10 12 14
Full Scale 9533 cts Cursor: 0.000
keV
(b)
20 µm
EHT = 5.00 kV
WD = 6.2 mm
Signal A = SE2
Mag = 500 X
Date :22 Nov 2013
Time :18:38:45
ZEISS
Spectrum 1
(b$_1$)
C
O
0 2 4 6 8 10 12 14
Full Scale 400 cts Cursor: 0.000
keV
Spectrum 1
(c)
300µm
Electron Image 1
Spectrum 1
(C$_1$)
C
O
P
Cl
0 2 4 6 8 10 12 14
Full Scale 2960 cts Cursor: 0.000
keV

Fig. 5

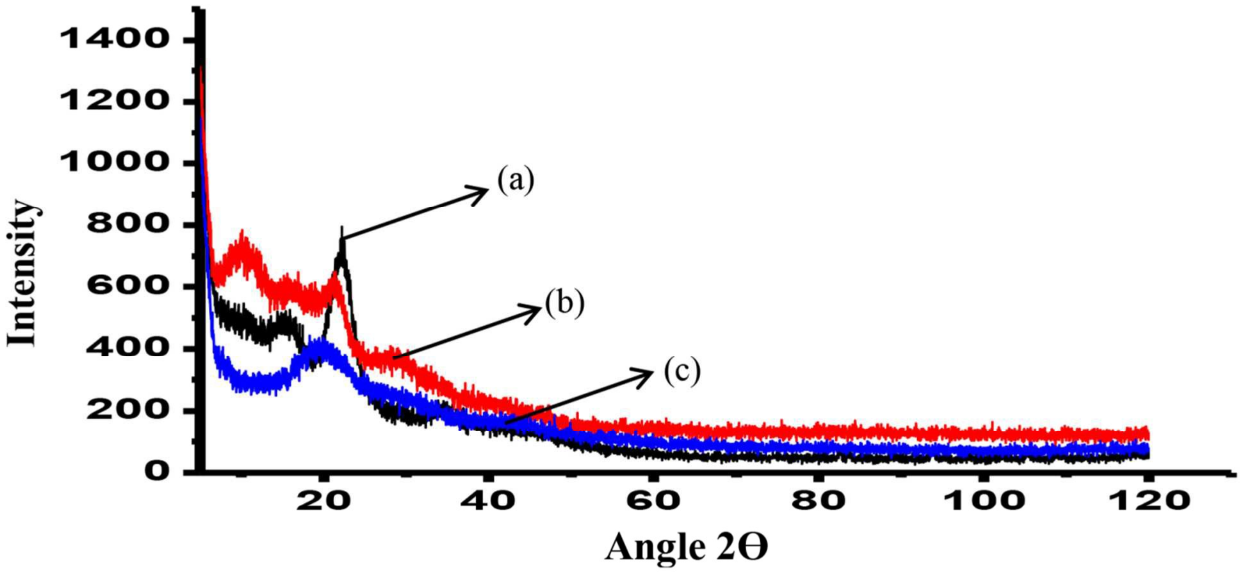
1400
1200
1000
800
600
400
200
0
Intensity
20
40
60
80
100
120
Angle 2Θ
(a)
(b)
(c)

Fig. 6

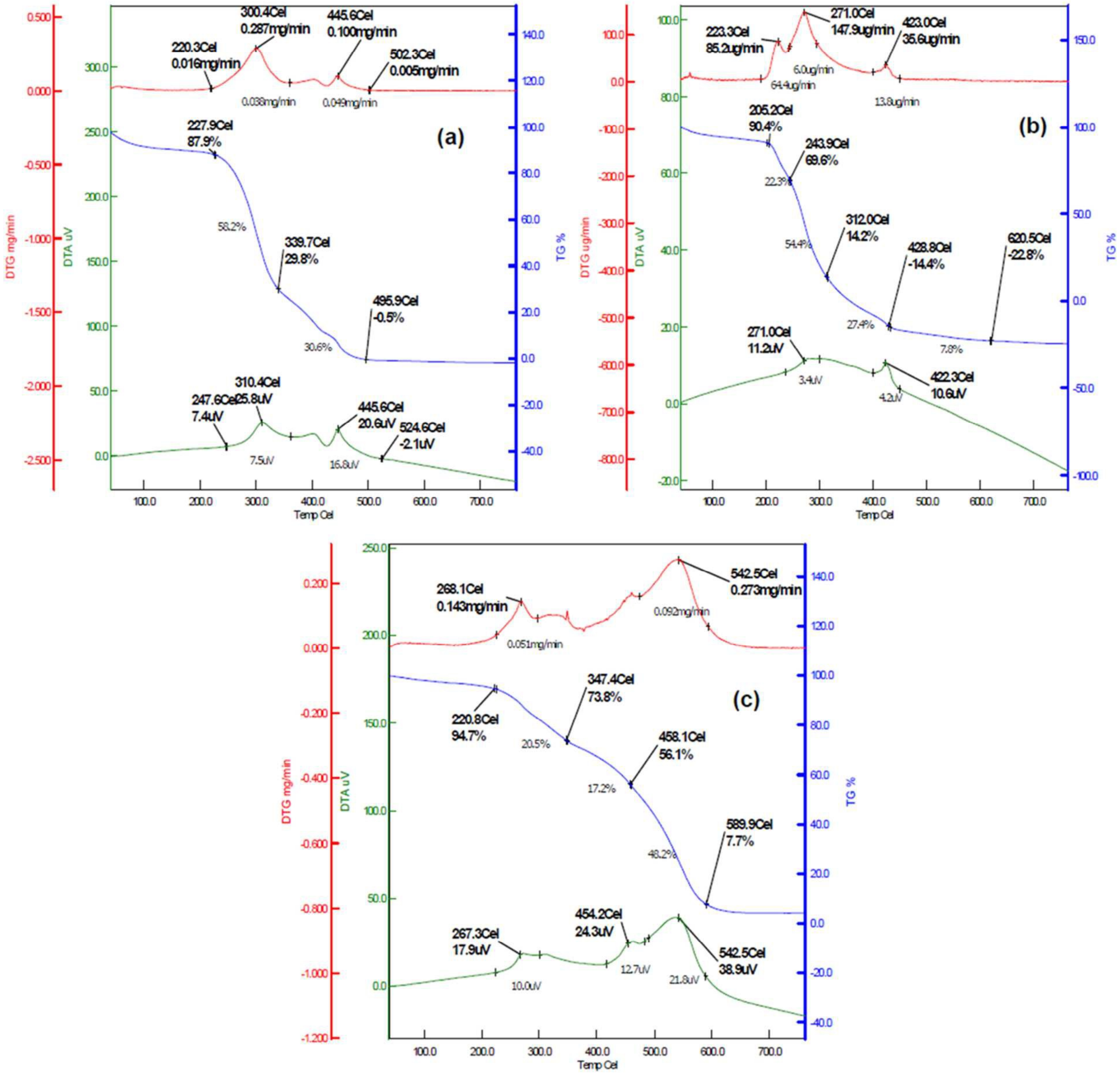
(a)
300.4Cel 0.287mg/min
445.6Cel 0.100mg/min
220.3Cel 0.016mg/min
502.3Cel 0.005mg/min
0.038mg/min
0.049mg/min
227.9Cel 87.9%
58.2%
339.7Cel 29.8%
495.9Cel -0.5%
30.6%
310.4Cel 25.8uV
247.6Cel 7.4uV
445.6Cel 20.6uV
524.6Cel -2.1uV
7.5uV
16.8uV
DTG mg/min
DTA uV
TG %
Temp Cel
(b)
271.0Cel 147.9ug/min
223.3Cel 85.2ug/min
423.0Cel 35.6ug/min
6.0ug/min
64.4ug/min
13.8ug/min
205.2Cel 90.4%
243.9Cel 69.6%
22.3%
54.4%
312.0Cel 14.2%
428.8Cel -14.4%
620.5Cel -22.8%
27.4%
7.8%
271.0Cel 11.2uV
3.4uV
422.3Cel 10.6uV
4.2uV
DTG ug/min
DTA uV
TG %
Temp Cel
(c)
268.1Cel 0.143mg/min
542.5Cel 0.273mg/min
0.092mg/min
0.051mg/min
220.8Cel 94.7%
347.4Cel 73.8%
20.5%
458.1Cel 56.1%
17.2%
589.9Cel 7.7%
48.2%
267.3Cel 17.9uV
454.2Cel 24.3uV
542.5Cel 38.9uV
10.0uV
12.7uV
21.8uV
DTG mg/min
DTA uV
TG %
Temp Cel

Fig 7

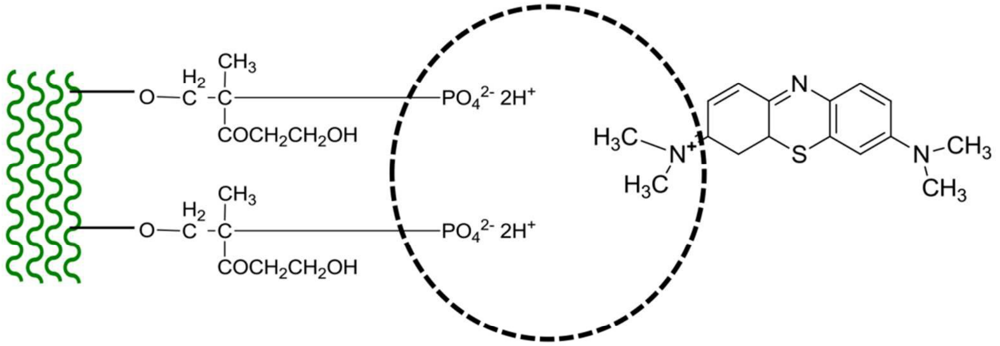

(8)

$$\text{MHa-g-poly(HEMA)-PO}_4^{2-}\,2\text{H}^+ + 2\text{MB}^+ \longrightarrow \text{MHa-g-poly(HEMA)-PO}_4^{2-}\,2\text{MB}^+ + 2\text{H}^+ \qquad (9)$$

$$\text{X}-\text{PO}_4^{2-}2\text{H}^+ \longrightarrow \text{X}-\text{PO}_4^{4-} + 2\text{H}^+ \qquad (10)$$

$$\text{X}-\text{PO}_4^{4-} + 2\text{MB}^+ \longrightarrow \text{X}-\text{PO}_4^{2-}2\text{MB}^+ \qquad (11)$$

$$\text{X}-\text{PO}_4^{2-}2\text{H}^+ + 2\text{MB}^+ \longrightarrow \text{X}-\text{PO}_4^{2-}2\text{MB}^+ + 2\text{H}^+ \qquad (12)$$

$$\text{X}-\text{PO}_4^{2-}2\text{H}^+ + 2\text{H}^+ \longrightarrow \text{X}-\text{PO}_4^{2-}4\text{H}^+ \qquad (13)$$

$$\text{X}-\text{PO}_4^{2-}4\text{H}^+ + 2\text{MB}^+ \longrightarrow \text{X}-\text{PO}_4^{2-}2\text{H}^+2\text{MB}^+ + 2\text{H}^+ \qquad (14)$$

$$\text{H}^+ + \text{OH}^- \longrightarrow \text{H}_2\text{O} \qquad (15)$$

Where X represents MHa-g-poly(HEMA)

Fig. 8

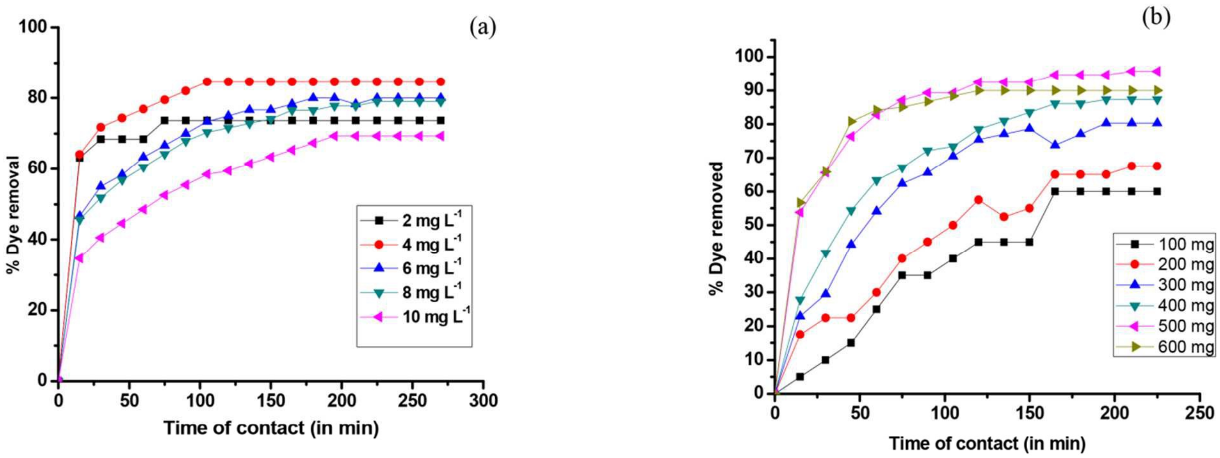
(a)
% Dye removal
Time of contact (in min)
0
20
40
60
80
100
0
50
100
150
200
250
300
2 mg L^{-1}
4 mg L^{-1}
6 mg L^{-1}
8 mg L^{-1}
10 mg L^{-1}
(b)
% Dye removed
Time of contact (in min)
0
10
20
30
40
50
60
70
80
90
100
0
50
100
150
200
250
100 mg
200 mg
300 mg
400 mg
500 mg
600 mg

Fig. 9

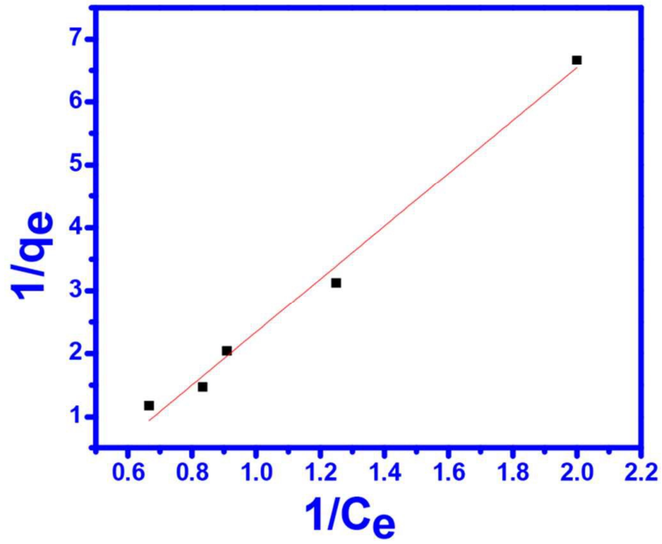

Fig. 10

Table 1: Comparitive study of the graft copolymerization of HEMA onto cellulosics vis-a-vis MHa-g-poly(HEMA)

Sr. No.	Graft Copolymer	%Grafting	References
1.	CMCH-g-HEMA	201.2	[100]
2	CMC-g-HEMA	397.0	[101]
3	CMCs-g-HEMA	857.0	[102]
4.	MHa-g-poly(HEMA)	422.0	[Present study]

Table 2: Ion-exchange capacity of various exchanging ions on phosphate cation-exchanger

Exchanging Ions	pH	Ionic Radii (A^0) [53]	Hydrated Ionic Radii(A^0) [53]	Ion-Exchange Capacity (m mol g^{-1})
Li^+	6.70	0.68	3.40	0.97
Na^+	6.70	0.97	2.76	1.31
K^+	6.80	1.33	2.32	1.42
Mg^{2+}	6.50	0.78	7.00	1.37
Ca^{2+}	6.50	1.06	6.30	0.91
Sr^{2+}	6.30	1.27	--	0.86

Table 3: Comparison between the ion-exchange capacity of various cation exchangers vis-a-vis MHa-g-poly(HEMA)$PO_4^{2-}2H^+$ cation exchanger

Sr. No.	Cation exchanger	IEC (mmol g^{-1})	References
1.	Nylon-6,6, Zr(IV) phosphate	1.90	[53]
2	Poly(methyl methacrylate) Zr(IV) phosphate	2.54	[103]
3	Acrylamide zirconium (IV) arsenate	1.63	[104]
4	Poly-o-toluidine Ce(IV) phosphate	1.07	[105]
5.	Acetate–tin (IV) phosphate	1.48	[106]
6.	Nylon-6,6 Sn(IV) Phosphate	1.98	[107]
7.	MHa-g-poly(HEMA)$PO_4^{2-}2H^+$	1.42	Present study

Table 4: Comparison between the atomic percentage of MHa, MHa-g-poly(HEMA) and MHa-g-poly(HEMA)$PO_4^{2-}2H^+$

Sr. No.	Sample name	Carbon (%)	Oxygen (%)	Phosphorous (%)
1	MHa	52.97	47.03	Nil
2	MHa-g-poly(HEMA)	57.19	42.81	Nil
3	MHa-g-poly(HEMA)$PO_4^{2-}2H^+$	72.71	23.86	3.21

Table 5: Comparative study of the effect of grafting of HEMA onto bio-polymers on % crystallinity vis-a-vis MHa-g-poly(HEMA) and cellulosics

Sr. No.	Bio-polymer	%Cr	References
1.	Cellulose	51-64%	[110]
2	Cellulose	56-78 %	[111]
4	HaC-g-poly(HEMA)	35.04 %	[112]
5	Cellulose	47.27%	Present study
6.	MHa-g-poly(HEMA)	43.43%	Present study

Where, %Cr = percentage crystallinity

Table 6: Thermal studies of MHa, graft copolymer and cation exchanger

Sample Code	TGA			DTA	DTG
	IDT (^{O}C)	FDT (^{O}C)	Residue left (%)	Exothermic peak at ^{O}C (μV)	Rate of wt. loss in mg min^{-1} (^{O}C)
MHa Fiber	227.9	495.9	-	310.4 (25.8) 445.6 (20.6)	0.287 (300.4) 0.100 (445.6)
MHa-g-poly(HEMA)	205.2	428.8	-	271.0 (11.2) 422.3 (10.6)	85.2 (223.3) 35.6 (423.0)
MHa-g-poly(HEMA)PO_4^{2-} $2H^+$	220.8	589.9	7.7	267.3 (17.9) 542.5 (38.9)	0.143 (268.1) 0.273 (542.5)

Table 7: Parameters of Langmuir isotherm

Sample name	Calculated values			
	q_m (mg g^{-1})	K_L (L mg^{-1})	R^2	R_L
MHa-g-poly(HEMA)$PO_4^{2-}2H^+$	3.12	0.076	0.9881	0.767